Measurement of IEC Groups and Subgroups Using Advanced Spectrum Estimation Methods

Antonio Bracale, *Member, IEEE*, Guido Carpinelli, *Member, IEEE*, Zbigniew Leonowicz, *Member, IEEE*, Tadeusz Lobos, and Jacek Rezmer

***Abstract*—The International Electrotechnical Commission (IEC) standards characterize the waveform distortions in power systems with the amplitudes of harmonic and interharmonic groups and subgroups. These groups/subgroups utilize the waveform spectral components obtained from a fixed frequency-resolution discrete Fourier transform (DFT). Using the IEC standards allows for a compromise among the different goals, such as the needs for accuracy, simplification, and unification. In some cases, however, the power-system waveforms are characterized by spectral components that the DFT cannot capture with enough accuracy due to the fixed frequency resolution and/or the spectral leakage phenomenon. This paper investigates the possibility of a group/subgroup evaluation using the following advanced spectrum estimation methods: adaptive Prony, estimation of signal parameters via rotational invariance techniques, and root MUltiple-SIgnal Classification (MUSIC). These adaptive methods use variable lengths of time windows of analysis to ensure the best fit of the waveforms; they are not characterized by the fixed frequency resolution and do not suffer from the spectral leakage phenomenon. This paper also presents the results of the applications of these methods to three test waveforms, to current and voltage waveforms obtained from simulations of a real dc arc-furnace plant, and to waveforms measured at the point of common coupling of the low-voltage network supplying a high-performance laser printer.**

***Index Terms*—DC arc furnaces, discrete Fourier transform (DFT), estimation of signal parameters via the rotational invariance techniques (ESPRIT) method, Prony method, root MUltiple-SIgnal Classification (MUSIC) method, spectrum estimation, subspace methods, waveform-distortion analysis.**

I. Introduction

THE QUALITY of voltage waveforms is an important issue for power-system utilities, electric-energy users, and manufacturers of electronic equipment. The main reasons for this are the increasing number of power-quality (PQ) problems linked to modern electronic devices, the susceptibility of loads to these problems, and the new liberalized competitive markets where electric disturbances can have significant economic consequences. Among the possible PQ disturbances, the proliferation of the nonlinear loads connected to the power systems has triggered the most concern for waveform distortions.

It is commonly known that several indices have been used to characterize waveform distortions. They generally refer to periodic signals, which allow for an "exact" definition of harmonic components and require only a single numerical value to characterize the disturbances. However, when the spectral components are time varying in amplitude, and/or in frequency, as in the case of nonstationary signals, a misleading use of the term "harmonic" can arise. Because of this, several numerical values are needed to characterize the time-varying nature of each spectral component of the signal [1], [2].

In addition, the standards and recommendations contain indices to characterize waveform distortions in power systems, as well as measurement methods and interpretation of results. In particular, the International Electrotechnical Commission (IEC) standards [3], [4] introduce specified signal processing recommendations and definitions. For practical purposes, they define the harmonic and interharmonic frequencies as integer and noninteger multiples of the fundamental frequency, respectively. With reference to a discrete Fourier transform (DFT), using a time window of ten (50 Hz) or 12 (60 Hz) fundamental periods, the IEC introduces the concept of harmonic and interharmonic groups and subgroups. The waveform distortions are then characterized by the amplitudes of these groupings versus time.

The crucial drawback of the DFT method is that the length of the window is related to the frequency resolution. Moreover, to ensure the accuracy of the DFT, the sampling interval of analysis should be an exact integer multiple of the waveform fundamental period [5].

In this paper, we propose to estimate the IEC groups and subgroups with some advanced spectrum estimation methods based on the Prony, the estimation of signal parameters via rotational invariance techniques (ESPRIT), and the root MUltiple-SIgnal Classification (MUSIC) parametric methods [6]–[11]. The Prony method approximates the sampled data with a linear combination of exponentials. It has a close relationship with the least squares linear prediction algorithms used for auto regressive and auto regressive moving average parameter estimation. The ESPRIT and root-MUSIC methods are based on the linear algebraic concepts of subspaces and have therefore been called as the "subspace methods." The model of the signal, in this case, is a sum of sinusoids in the background of noise of a known covariance function.

All of the considered parametric methods use signal models in which the time-window length of analysis is unknown.

Manuscript received July 15, 2006; revised October 21, 2007. This work was supported in part by the Ministry of Education and Science of Poland under Grant 3T10A04030.

A. Bracale and G. Carpinelli are with the Electrical Engineering Department, University of Naples "Federico II," 80100 Naples, Italy (e-mail: antonio.bracale@ieee.org; guido.carpinelli@unina.it).

Z. Leonowicz, T. Lobos, and J. Rezmer are with the Electrical Engineering Department, Wroclaw University of Technology, 50370 Wroclaw, Poland (e-mail: tadeusz.lobos@pwr.wroc.pl).

Color versions of one or more of the figures in this paper are available online at http://ieeexplore.ieee.org.

Digital Object Identifier 10.1109/TIM.2007.911701

Bracale *et al.* [7] propose an adaptive technique that was successfully applied to the Prony method. This technique allows us to evaluate the time-window length of analysis, ensuring the best fit of the signal variations. In this paper, the adaptive technique proposed in [7] is applied to the ESPRIT and root-MUSIC methods to obtain the adaptive ESPRIT and adaptive root-MUSIC methods, respectively.

The novelty of the proposed approach lies in replacing the DFT with advanced spectrum estimation methods, which gives more accurate results when analyzing strongly distorted waveforms with nonstationary behavior. Other approaches exist in the literature, which aim to avoid or diminish the inherent drawbacks of the DFT (e.g., wavelets, filters, or windowing techniques). Recently, significant improvements have also been proposed in [12]–[14].

In particular, the approach presented in this paper demonstrates significant advantages in terms of waveform approximation and has been evaluated on test waveforms, on waveforms obtained from simulations of a real dc arc-furnace plant, and on waveforms measured at the point of common coupling (PCC) of the low-voltage (LV) network supplying a high-performance laser printer.

The proposed adaptive Prony, ESPRIT, and root-MUSIC methods have the following features.

1) The time windows of analysis can have variable lengths, ensuring the best fit of the time-varying waveforms.
2) The time-window length does not constrain the frequency resolution.
3) They do not suffer from the spectral leakage phenomenon.

This paper is organized such that the definitions of the IEC groups and subgroups are briefly recalled. Then, the proposed adaptive Prony, ESPRIT, and root-MUSIC methods are described. Finally, the results of the numerical applications are reported and discussed.

This paper is an extended version of the paper [15] presented at the 2006 Instrumentation and Measurement Technology Conference.

II. Proposed Approach

The adaptive Prony, ESPRIT, and root-MUSIC methods (for the descriptions of the methods, see Sections II-A–C, respectively) are compared with the DFT on the basis of the values of the IEC harmonic and interharmonic groups/subgroups (Fig. 1).

As commonly known [3], the amplitudes of the IEC harmonic and interharmonic subgroups $G_{\mathrm{sg},n}$ and $C_{\mathrm{isg},n}$ can be evaluated, respectively, as

$$G^2_{\mathrm{sg},n} = \sum_{k=-1}^{1} C^2_{10n+k}$$
$$C^2_{\mathrm{isg},n} = \sum_{k=2}^{8} C^2_{10n+k} \tag{1}$$

where C_{10n+k} refers to the spectral components (rms value) of the DFT output, using a window width of ten fundamental periods (as in the case of a 50-Hz system, which is used in this paper).

The amplitudes of the harmonic and interharmonic groups $G_{\mathrm{g}-n}$ and $C_{\mathrm{ig}-n}$ can be evaluated, respectively, as

$$G^2_{\mathrm{g},n} = \frac{C^2_{10n-5}}{2} + \sum_{k=-4}^{4} C^2_{10n+k} + \frac{C^2_{10n+5}}{2}$$
$$C^2_{\mathrm{ig},n} = \sum_{k=1}^{9} C^2_{10n+k} \tag{2}$$

where C_{10n+k} denotes the aforementioned spectral components (rms value) of the DFT output.

Finally, the results are smoothed over 15 intervals of ten fundamental periods. In other words, the results are smoothed over the entire interval of several very short time measurements [4].

In the next section, the adaptive Prony, ESPRIT, and root-MUSIC methods are presented (Sections II-A–C, respectively). Then, we show how the relationship between (1) and (2) should be modified in the framework of the proposed methods (Sections II-D and E).

A. Adaptive Prony Method

Let us consider a time-window length including N samples $[x_1\ x_2\ \cdots\ x_N]$ of the investigated waveform; the Prony method approximates each sample using the following linear combination of M exponential functions:

$$\hat{x}(t_n) = \sum_{k=1}^{M} A_k e_k^{(\alpha_k + j\omega_k)(n-1)T_s + j\phi_k} \tag{3}$$

where $n = 1, 2, \ldots, N$, T_s is the sampling period, A_k is the amplitude, α_k is the damping factor, ω_k is the angular velocity, ϕ_k is the initial phase, and k is the exponential code.

The Toeplitz matrix created from the samples makes it possible to determine the vector of coefficients $\boldsymbol{a}$ of the characteristic polynomial

$$z^M + a_1 z^{M-1} + \cdots + a_{M-1} z + a_M = 0. \tag{4}$$

The roots of the characteristic polynomial define the Vandermonde matrix

$$\mathbf{Z} = \begin{bmatrix} \mathbf{z}_1^0 & \cdots & \mathbf{z}_{M-1}^0 & \mathbf{z}_M^0 \\ \mathbf{z}_1^1 & \cdots & \mathbf{z}_{M-1}^1 & \mathbf{z}_M^1 \\ \vdots & \vdots & \vdots & \vdots \\ \mathbf{z}_1^{M-1} & \cdots & \mathbf{z}_{M-1}^{M-1} & \mathbf{z}_M^{M-1} \end{bmatrix}. \tag{5}$$

The vector of complex values $\mathbf{H}$ can be calculated from

$$\mathbf{Z} \cdot \mathbf{H} = \mathbf{X} \tag{6}$$

where

$$\mathbf{X} = [\, x_1 \quad x_2 \quad \cdots \quad x_M \,].$$

The parameters of the exponential components for $k = 1, 2, \ldots, M$ can be calculated using the following relations: $A_k = |\mathbf{h}_k|, \alpha_k = f_\mathrm{s} \cdot \ln|\mathbf{z}_k|, \omega_k = f_\mathrm{s} \cdot \arg(\mathbf{z}_k)$, and $\phi_k = \arg(\mathbf{h}_k)$, where f_s is the sampling frequency.

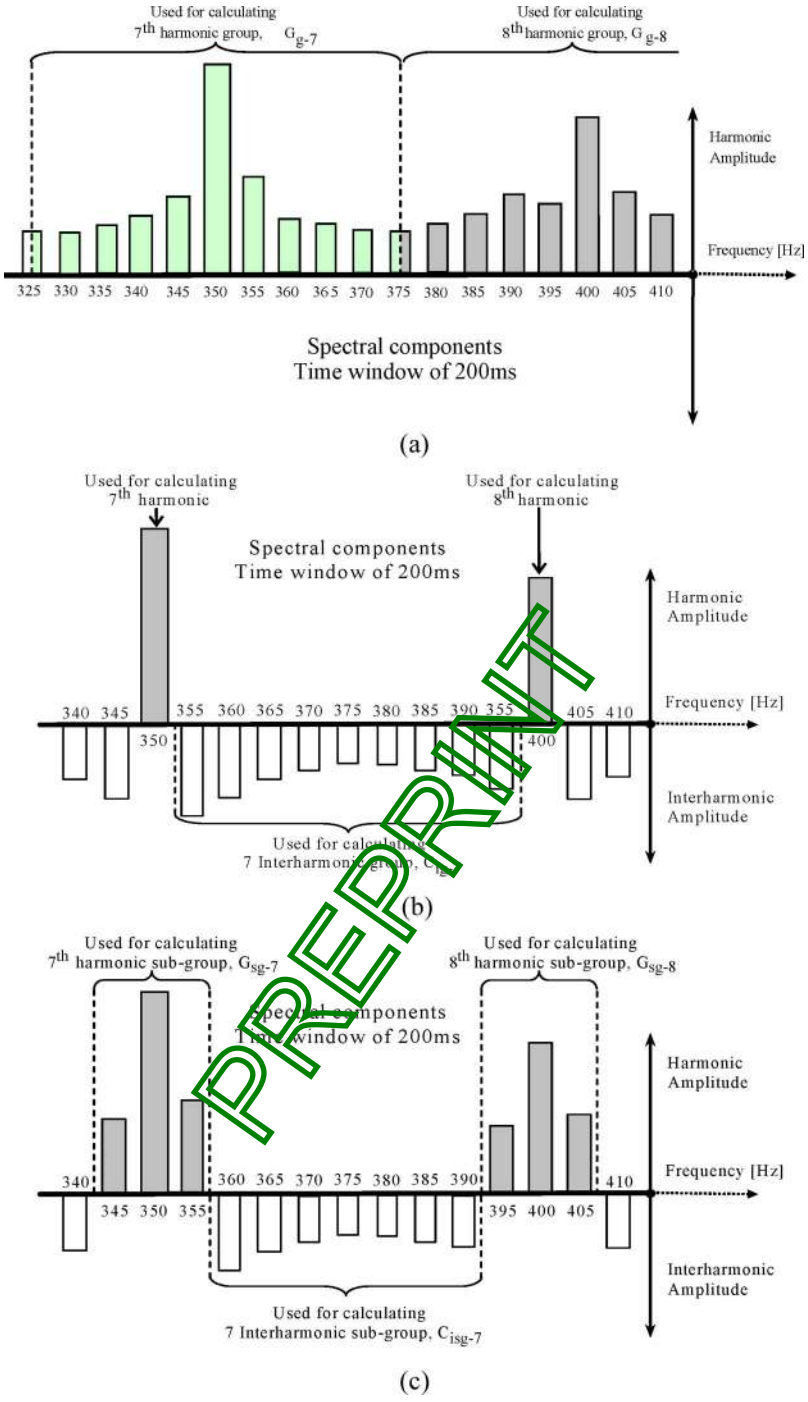

Fig. 1. IEC harmonic ↑ and interharmonic ↓ groupings. (a) Harmonic groups, (b) interharmonic groups, and (c) harmonic and interharmonic subgroups.

The adaptive Prony method is a modified version of the Prony method proposed in [7]. The basic idea of the adaptive Prony method consists of applying the Prony method to a number of "short contiguous time windows" inside the ten fundamental periods. The lengths of these short time windows are variable; this variability ensures the best fit of the signal variations along the ten fundamental periods of the waveform.

Next, we present the adaptive technique proposed in [7]. Let us consider the signal $x(t)$ and the L samples of the generic jth short time window, which are obtained using the sampling frequency $f_s = 1/T_s$. For each sample, the following estimation error can be introduced:

$$e_n = |\hat{x}(t_n) - x(t_n)| \tag{7}$$

where $t_n = nT_s (n = 1, 2, 3, \ldots, L)$, and $\hat{x}(t_n)$ is given by (3).

Applying (3) for all L samples, the following mean-square relative error can be defined:

$$\varepsilon^2_{\text{curr}}(j) = \frac{1}{L} \sum_{n=1}^{L} \frac{|\hat{x}(t_n) - x(t_n)|^2}{x(t_n)^2}. \tag{8}$$

This mean-square relative error gives a measure of the fidelity of the model considered. By defining a threshold $\varepsilon^2_{\rm thr}$ (an acceptable mean-square relative error), it is possible to choose a length for the short time window (and then a subset of the data segment length), ensuring a satisfactory approximation ($\varepsilon^2_{\rm curr} \leq \varepsilon^2_{\rm thr}$).

In practice, the adaptive technique applies the following iterative algorithm inside the signal $x(t)$ of duration $T_{\rm obs}$.

1) Select a starting short-time-window length $T_{\rm min}$.
2) Apply the Prony method to the samples in the short time window to obtain the model parameters (amplitudes, damping factors, frequencies, and initial phases of the Prony exponentials).
3) Use the exponentials obtained in step 2) to calculate $\varepsilon^2_{\rm curr}$ with (8).
4) Compare $\varepsilon^2_{\rm curr}$ with the threshold $\varepsilon^2_{\rm thr}$, and observe the following.
   a) If $\varepsilon^2_{\rm curr} \leq \varepsilon^2_{\rm thr}$, store the Prony-model exponential parameters, and increase the short-time-window width (and then the subset of the data segment) until $\varepsilon^2_{\rm curr} \leq \varepsilon^2_{\rm thr}$ and $t_{\rm f} \leq T_{\rm obs}$, and then, go to step 5).
   b) If $\varepsilon^2_{\rm curr}$ is greater than the threshold $\varepsilon^2_{\rm thr}$, increase the short-time-window width, and then, go to step 6).
5) Store the short-time spectral components, and select a new starting short-time-window width.
6) Compare $t_{\rm f}$ with $T_{\rm obs}$. If $t_{\rm f}$ is less than or equal to $T_{\rm obs}$, go to step 2). If $t_{\rm f}$ is greater than $T_{\rm obs}$, then store the spectral components for all the short contiguous time windows, and stop the algorithm.

It should be noted that, in step 4a), the short-time window length is increased until the condition $\varepsilon^2_{\rm curr} \leq \varepsilon^2_{\rm thr}$ is satisfied; the Prony-model parameters remain fixed at the values that satisfy the criterion for the first time. In this way, a nonnegligible reduction of the computational efforts arises, mainly in the presence of slight time-varying waveforms.

Also note that, for the model-parameter calculation in each short time window in step 2), the number of components M has to be selected since this number is an input parameter for the model reported in (3). As shown in [5] and [6], choosing the number of components is a well-known problem in the field of signal processing. In [8], several criteria are compared, such as the final prediction error, the Akaike's information criterion, the minimum description-length criterion, the autoregressive transfer criterion, and a criterion based on the eigendecomposition of the sample autocorrelation matrix. In [8], the MDL criterion is shown as an appropriate method to evaluate the optimal number of components in the case of power-system waveform distortions. This method is based on the selection of the M value corresponding to the minimum of the MDL function, which is defined as follows:

$$\mathrm{MDL}(M) = N \ln\left(\hat{\sigma}^2_M\right) + M \ln(N) \tag{9}$$

where N is the number of time-window samples, and $\hat{\sigma}^2_M$ is the estimated variance of the square prediction error.

B. Adaptive ESPRIT Method

The original ESPRIT algorithm [5] is based on naturally existing shift invariance between the discrete time series, which leads to rotational invariance between the corresponding signal subspaces. The assumed signal model is as follows:

$$\hat{x}(n) = \sum_{k=1}^{M} A_k e_k^{(j\omega_k n)} + w(n) \tag{10}$$

where $w(n)$ represents the additive noise. The eigenvectors $\mathbf{U}$ of the autocorrelation matrix of the signal define two subspaces (signal and noise subspaces) by using two selector matrices Γ_1 and Γ_2 such that

$$\mathbf{S}_1 = \Gamma_1 \mathbf{U} \quad \mathbf{S}_2 = \Gamma_2 \mathbf{U}. \tag{11}$$

The rotational invariance between both subspaces leads to the equation

$$\mathbf{S}_1 = \Phi \mathbf{S}_2 \tag{12}$$

where

$$\mathbf{\Phi} = \begin{bmatrix} e^{\mathrm{j}\omega_1} & 0 & \cdots & 0 \\ 0 & e^{\mathrm{j}\omega_2} & \cdots & 0 \\ \vdots & \vdots & \ddots & \vdots \\ 0 & 0 & \cdots & e^{\mathrm{j}\omega_{\mathrm{M}}} \end{bmatrix}. \tag{13}$$

The matrix $\mathbf{\Phi}$ contains all information about the frequencies of M components. Additionally, the total least squares approach assumes that both estimated matrices $\mathbf{S}$ can contain errors and also finds the matrix $\mathbf{\Phi}$ as a minimization of the Frobenius norm of the error matrix. The amplitudes of the components can be found in a similar way as the Prony method by using (10).

In this paper, the adaptive technique proposed in [7] has also been applied to the ESPRIT method. In order to obtain the adaptive ESPRIT method, this technique is applied to a number of "short contiguous time windows." Since the ESPRIT method does not provide any phase estimation of the spectral component, the short contiguous time windows are obtained by minimizing the error between the actual waveform energy content evaluated in the time domain and the estimated waveform energy content obtained using the spectral components in the frequency domain. This approach results in the adaptive ESPRIT method.

C. Adaptive Root-MUSIC Method

The MUSIC method [5] involves the projection of the signal vector onto the entire noise subspace. The matrices of the eigenvectors of the autocorrelation matrix $\mathbf{R}_x$ can be divided into signal and noise matrices

$$\mathbf{E}_{\rm signal} = \lfloor\, \mathbf{e}_1 \quad \mathbf{e}_2 \quad \cdots \quad \mathbf{e}_p \,\rfloor \tag{14}$$

$$\mathbf{E}_{\rm noise} = \lfloor\, \mathbf{e}_{p+1} \quad \mathbf{e}_{p+2} \quad \cdots \quad \mathbf{e}_M \,\rfloor. \tag{15}$$

Similarly, two matrices of eigenvalues $\mathbf{\Lambda}_{\text{signal}}$ and $\mathbf{\Lambda}_{\text{noise}}$ can be built. It is possible then to rewrite $\mathbf{R}_x$ as

$$\mathbf{R}_x = \mathbf{E}_{\text{signal}}\Lambda_{\text{signal}}\mathbf{E}^{*T}_{\text{signal}} + \mathbf{E}_{\text{noise}}\Lambda_{\text{noise}}\mathbf{E}^{*T}_{\text{noise}}. \quad (16)$$

The MUSIC method uses only the noise subspace for the estimation of the frequencies of the sinusoidal component, whereas the ESPRIT method uses only the signal subspace. $\mathbf{E}_{\text{noise}}$ can be used to form the polynomial

$$\hat{P}^{-1}(z) = \sum_{i=p+1}^{M} E_i(z)E_i^*(1/z) \quad (17)$$

which has p double roots lying on the unit circle. These roots also correspond to the frequencies of the signal components. This technique for finding the frequencies is therefore called the root-MUSIC method.

After the frequencies are calculated, the powers of each component can be estimated from the eigenvalues and the eigenvectors of the correlation matrix [5].

As with the ESPRIT method, the root-MUSIC method does not provide any phase estimation of the spectral component. The most adequate "short contiguous time windows" are obtained by minimizing the error between the actual waveform energy content evaluated in the time domain and the estimated waveform energy content obtained using the spectral components in the frequency domain. This approach results in the adaptive root-MUSIC method.

D. Calculation of the Short Harmonic and Interharmonic Subgroup Amplitudes

All advanced methods recalled in the previous sections permit the evaluation of the spectral components of the distorted waveforms inside the short contiguous time windows. Therefore, the need to define the corresponding "short-time harmonic and interharmonic subgroups" arises. These can be defined as the subgroups calculated for a short time window. With reference to the jth short time window, they are given as

$$G^2_{\text{ssg},n}(j) = \sum_{k=1}^{M_{\text{nsg}}} C_k^2(j)$$

$$C^2_{\text{issg},n}(j) = \sum_{k=1}^{M_{\text{nisg}}} C_k^2(j) \quad (18)$$

where C_k is the amplitude (rms value) of the spectral components, M_{nsg} is the number of spectral components inside the frequency interval $[nf_1 - 7.5, nf_1 + 7.5]$ Hz, and M_{nisg} is the number of spectral components inside the frequency interval $[nf_1 + 7.5, (n+1)f_1 - 7.5]$ Hz. With reference to the IEC intervals, the need to enlarge the frequency ranges for both harmonic and interharmonic grouping evaluations is derived from the absence of the DFT fixed frequency resolution in the advanced method applications.

E. Calculation of the Harmonic and Interharmonic Subgroup Amplitudes

Once the short-time harmonic and interharmonic subgroups for all windows inside an interval of ten fundamental periods have been determined, the harmonic and interharmonic subgroup amplitudes can be calculated by averaging all of the aforementioned short harmonic and interharmonic subgroup amplitudes. This results in the equation

$$G^2_{\text{sg},n} = \frac{\sum_{j=1}^{N_w} N_W(j)G^2_{\text{ssg},n}(j)}{N_W}$$

$$C^2_{\text{isg},n} = \frac{\sum_{j=1}^{N_w} N_W(j)C^2_{\text{issg},n}(j)}{N_W} \quad (19)$$

where N_W is the number of samples inside the ten fundamental periods, and $N_W(j)$ is the number of samples in the jth short contiguous time window.

Finally, the results can be averaged over 15 intervals of the ten fundamental periods in order to obtain the results referred to the very short time measurements.

III. Numerical Applications

Several numerical experiments were performed. We report the results obtained from the analysis of three sample waveforms, the current and voltage waveforms at the medium-voltage (MV) busbar using a simulated dc arc-furnace plant [16], and the voltage waveform measured at the PCC of the LV network supplying a high-performance laser printer [14].

In the next three sections, the IEC method, adaptive root-MUSIC method, adaptive ESPRIT method, and adaptive Prony method are referred to as the IECM, ARM, AEM, and APM, respectively. In order to compare the distortion estimation of the proposed methods with the IECM, the harmonic and interharmonic subgroups were evaluated by applying the definitions reported in Sections II-D and E.

A. Test Waveforms

The sampling frequency for all experiments and methods was 5 kHz. The window width was $T_w = 200.00$ ms for the IECM. The acceptable mean-square relative error for all the adaptive methods was $\varepsilon = 1.0 \cdot 10^{-6}$.

Case Study 1: The considered signal is constituted by a tone of amplitude of 1 pu at a fundamental frequency of 50 Hz and an interharmonic tone of amplitude of 0.01 pu with a frequency varying between 58 and 65 Hz (in increments of 0.5 Hz) over 15 experiments.

Fig. 2 shows the IECM results in terms of the magnitude error for the interharmonic subgroup $C_{\text{isg},1}$ versus the frequency of the interharmonic component in the 15 experiments. The absolute errors of the IECM reach more than 5% under the worst conditions when the interharmonic tone is closest to the first harmonic-subgroup frequency interval. The error is null in the experiments characterized by interharmonic

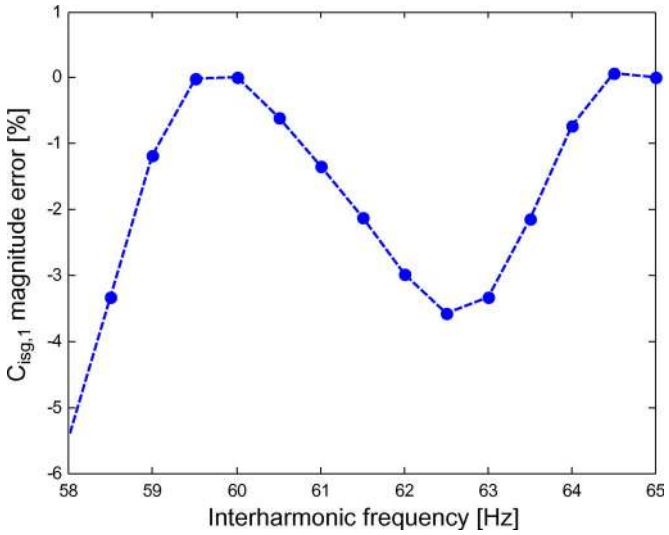

Fig. 2. Case study 1. Interharmonic subgroup $C_{\mathrm{isg},1}$ magnitude error (in percentage) versus interharmonic frequency obtained using the IECM (–●–).

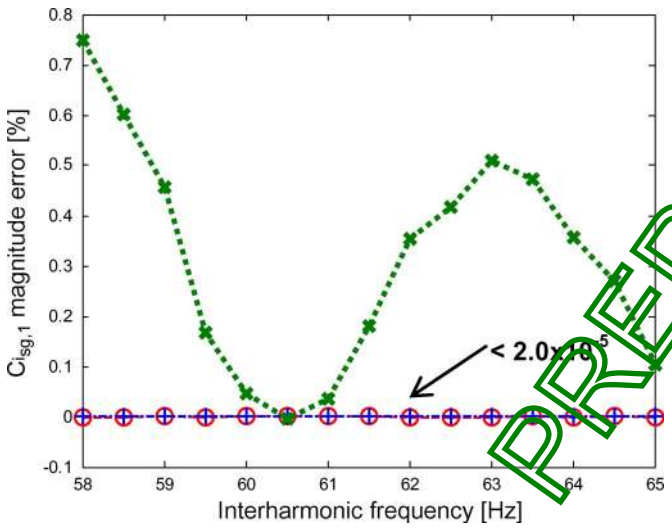

Fig. 3. Case study 1. Interharmonic subgroup $C_{\mathrm{isg},1}$ magnitude error (in percentage) versus interharmonic frequency obtained using the APM (–○–), ARM (–x–), and AEM (–+–).

frequencies of 60 and 65 Hz, where the interharmonic is synchronized with T_w.

Fig. 3 shows the results, which are obtained by applying the proposed adaptive methods, in terms of the magnitude error for the interharmonic subgroup $C_{\mathrm{isg},1}$ versus the frequency of the interharmonic component. In general, all of the adaptive methods provide a better approximation of the interharmonic subgroup $C_{\mathrm{isg},1}$ compared with those obtained by the IECM.

All adaptive methods provide a spectrum with only two components for all 15 experiments, showing the absence of spectral leakage phenomenon. The errors of APM and AEM do not reach $2.0 \times 10^{-5}\%$, and the APM generally gives the best performance. It should be noted that the results for the AEM and APM are not influenced by the frequency position of the interharmonic tone. Only ARM suffers from the proximity of the interharmonic tone to the first harmonic subgroup $(C_{\mathrm{isg},1})$; it gives varying errors in the interharmonic-tone amplitude estimation, causing varying errors in the subgroup $C_{\mathrm{isg},1}$ evaluation. Nonetheless, the ARM error is lower than 0.8%.

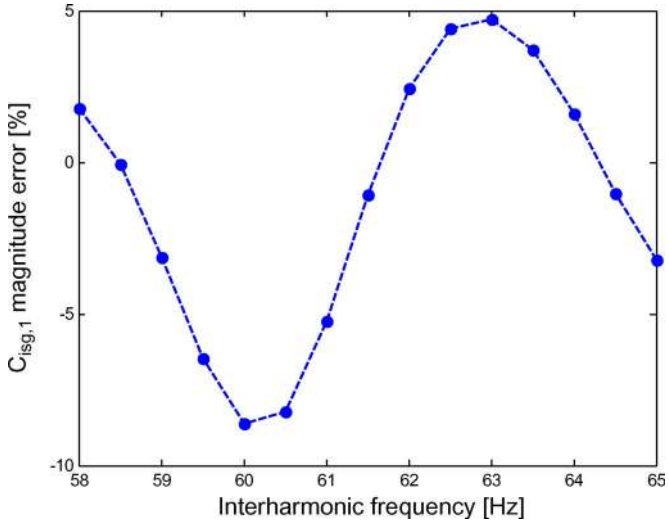

Fig. 4. Case study 2. Interharmonic subgroup $C_{\mathrm{isg},1}$ magnitude error (in percentage) versus interharmonic frequency obtained using the IECM (–●–).

Case Study 2: In the synchronization of the window width with the actual system fundamental frequency, a 0.03% maximum error in the window duration is permitted by the IEC standards [3]. Therefore, the presence of a fundamental tone frequency at 50.015 Hz introduces a further kind of desynchronization because the window width adopted for the IEC method remains equal to 200.00 ms.

In this case, the second signal considered is the same as in Section III-A1, except for the fundamental tone frequency, which is at 50.015 Hz.

Fig. 4 shows the IECM results in terms of the magnitude error for the interharmonic subgroup $C_{\mathrm{isg},1}$ versus the frequency of the interharmonic component in the 15 experiments. Comparing Figs. 2 and 4, we observe that the errors of the IECM increase, reaching values over -8.5% due to DFT spectral leakage. In this case, the desynchronization with the fundamental causes the presence of some high-amplitude "false" interharmonics in the DFT spectrum; the interference between these false interharmonics and the interharmonic tone of 0.01 pu changes with the frequency position of this last tone, causing changing subgroup $C_{\mathrm{isg},1}$ errors in the 15 experiments (Fig. 4).

Fig. 5 shows the results obtained by applying the proposed adaptive methods in terms of the magnitude error for the interharmonic subgroup $C_{\mathrm{isg},1}$ versus the frequency of the interharmonic component. All adaptive methods provide a spectrum with only two components. Comparing Figs. 3 and 5, it is possible to observe that, while the performances of APM and AEM remain very good with no reduction of approximation, the ARM errors increase, reaching a maximum value of 1.7%.

Moreover, the ARM gives errors in the interharmonic amplitude estimation, which are more stable than those resulting in Section III-A1; thus, the subgroup $C_{\mathrm{isg},1}$ errors slightly decrease, increasing the interharmonic-tone frequency.

Case Study 3: The signal considered is constituted by a tone of amplitude of 1 pu at a fundamental frequency of 50.015 Hz

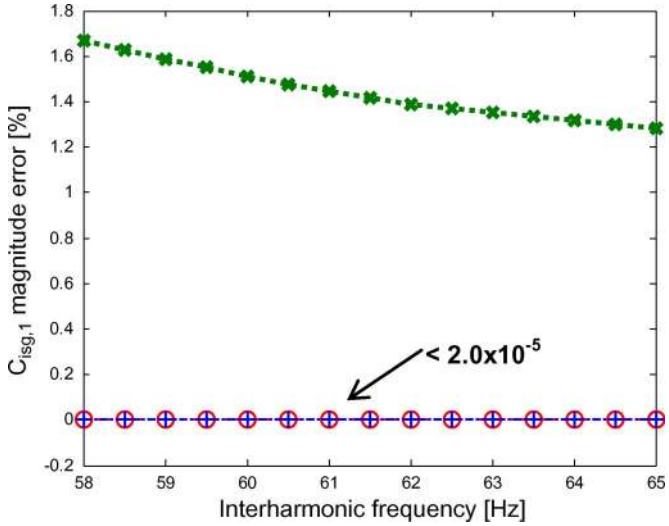

Fig. 5. Case study 2. Interharmonic subgroup $C_{\mathrm{isg},1}$ magnitude error (in percentage) versus interharmonic frequency obtained using the APM (–○–), ARM (–x–), and AEM (–+–).

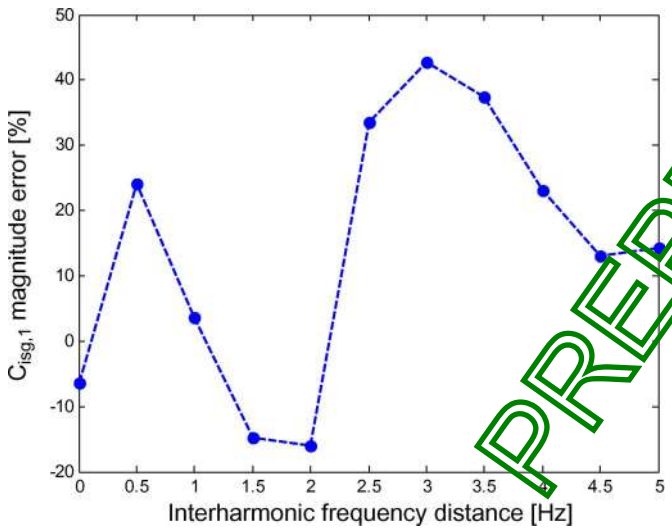

Fig. 6. Case study 3. Interharmonic subgroup $C_{\mathrm{isg},1}$ magnitude error (in percentage) versus interharmonic frequency obtained using the IECM (–●–).

and by a couple of interharmonic tones of amplitude of 0.01 pu located at symmetrical frequency positions from 60 Hz. The first starts from 60 Hz and varies its frequency to 65 Hz by increments of 0.5 Hz, whereas the second starts from 60 Hz and varies its frequency to 55 Hz by decrements of 0.5 Hz. Eleven experiments were performed.

Figs. 6 and 7 show the results obtained using the IECM and adaptive methods, respectively, in terms of the magnitude error for the interharmonic subgroup $C_{\mathrm{isg},1}$ versus the absolute value of the distance of each interharmonic component from 60 Hz in the 11 experiments.

From the analysis of Fig. 6, it should be noted that, in this case, the IECM greatly suffers from the interference problems between the two interharmonics due to their proximity. The IECM captures the spectral leakage due to the desynchronization of the fundamental and the interharmonics that are adjacent to the first interharmonic subgroup, which gives misleading results with errors greater than 40%.

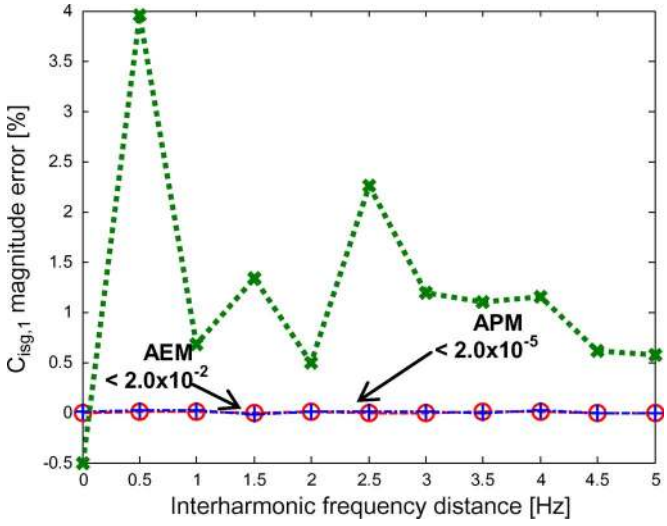

Fig. 7. Case study 3. Interharmonic subgroup $C_{\mathrm{isg},1}$ magnitude error (in percentage) versus interharmonic frequency obtained using the APM (–○–), ARM (–x–), and AEM (–+–).

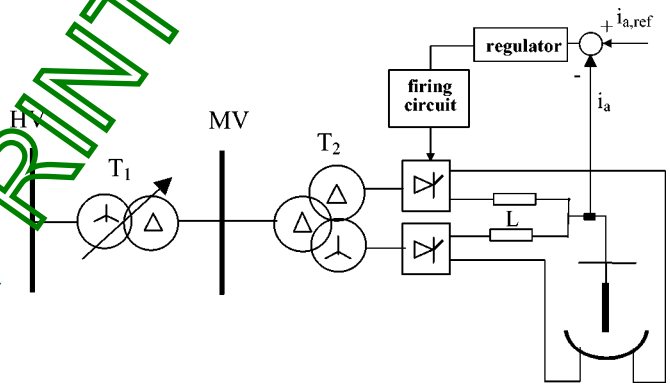

Fig. 8. Scheme of the dc arc furnace.

Once again, the proposed methods provide a spectrum with only three components for all 11 experiments, confirming the absence of spectral leakage phenomenon. By comparing Figs. 5 and 7, note that the ARM increases in errors. Once again, the ARM gives varying errors in the interharmonic amplitude estimation, in particular, these errors cause varying $C_{\mathrm{isg},1}$ magnitude errors, reaching its maximum error when the two interharmonic tones are closest (interharmonic distance of 0.5 Hz).

In contrast, the APM and AEM still give good results even if with a slight reduction of accuracy with respect to the previous case studies. In particular, for this example waveform, the APM gives the best approximation, ensuring an error that does not reach $2.0 \times 10^{-5}\%$.

B. DC Arc-Furnace Waveforms

The next investigated waveforms originate from the simulation of a real dc arc-furnace plant, the scheme of which is shown in Fig. 8. To simulate the dc arc behavior, a chaotic model has been applied [16].

In the dc arc furnaces, the presence of the ac/dc static converter and the random motion of the electric arc, whose

TABLE I
DC ARC-FURNACE CURRENT WAVEFORM: HARMONIC SUBGROUP AMPLITUDES EVALUATED OVER 3-S INTERVAL USING THE DIFFERENT TECHNIQUES

	$G_{sg,11}$ [A]	$G_{sg,12}$ [A]	$G_{sg,13}$ [A]
IECM	172.76	12.19	132.28
ARM	180.03	1.19	138.28
AEM	183.43	1.20	139.39
APM	181.10	1.07	135.39

TABLE II
DC ARC-FURNACE VOLTAGE WAVEFORM: HARMONIC SUBGROUP AMPLITUDES EVALUATED OVER 3-S INTERVAL USING THE DIFFERENT TECHNIQUES

	$G_{sg,11}$ [V]	$G_{sg,12}$ [V]	$G_{sg,13}$ [V]
IECM	335.30	26.83	333.89
ARM	351.12	2.68	348.45
AEM	352.26	2.71	349.24
APM	347.70	2.42	348.65

nonlinear and time-varying nature is known, are responsible for the dangerous perturbations, in particular the waveform distortions and the voltage fluctuations, which are time varying.

To compare the different adaptive techniques (the ARM, AEM, and APM) with the IEC method, the current and voltage waveforms at the MV busbar of the dc arc furnace are analyzed. For a better estimation of the spectral components, it was experimented to be useful the preprocessing of the data with proper filters.

The following filters have been applied:

1) a fourth-order band-stop Butterworth IIR filter that cuts out the main (50 Hz) component;
2) fourth-order bandpass Butterworth IIR filters centered at 550 and 650 Hz for the 11th and 13th harmonic subgroups, respectively.

The most significant harmonic subgroups of the current and voltage waveforms are reported in Tables I and II, respectively. The most significant interharmonic subgroups of the current and voltage waveforms are reported in Tables III and IV, respectively.

From the analysis of these tables, it clearly appears that, with reference to the current and voltage harmonic subgroup amplitudes, $G_{\mathrm{sg},11}$ and $G_{\mathrm{sg},13}$ (Tables I and II), ARM, APM, and AEM give higher values than those obtained using the IECM. Moreover, the IECM gives values of the current and voltage harmonic subgroups $G_{\mathrm{sg},12}$ that are significantly greater than those obtained with any of the adaptive techniques.

The IECM lower values for the harmonic subgroups $G_{\mathrm{sg},11}$ and $G_{\mathrm{sg},13}$, as well as the IECM higher values for the harmonic subgroup $G_{\mathrm{sg},12}$, are due to the spectral leakage present in

TABLE III
DC ARC-FURNACE CURRENT WAVEFORM: INTERHARMONIC SUBGROUP AMPLITUDES EVALUATED OVER 3-S INTERVAL USING THE DIFFERENT TECHNIQUES

	$C_{isg,10}$ [A]	$C_{isg,11}$ [A]	$C_{isg,12}$ [A]	$C_{isg,13}$ [A]
IECM	58.27	64.17	58.83	53.87
ARM	40.75	44.57	41.98	41.67
AEM	40.84	45.39	42.57	42.72
APM	40.29	45.16	39.35	37.77

TABLE IV
DC ARC-FURNACE VOLTAGE WAVEFORM: INTERHARMONIC SUBGROUP AMPLITUDES EVALUATED OVER 3-S INTERVAL USING THE DIFFERENT TECHNIQUES

	$C_{isg,10}$ [V]	$C_{isg,11}$ [V]	$C_{isg,12}$ [V]	$C_{isg,13}$ [V]
IECM	109.33	129.43	143.69	139.57
ARM	97.12	90.21	101.75	109.34
AEM	96.19	91.68	103.34	110.65
APM	86.77	84.48	99.51	108.39

the IECM algorithm. In fact, part of the energy content of the 11th and 13th harmonics is dispersed among the contiguous harmonic and interharmonic subgroups.

The proposed methods do not suffer at all from this problem. With reference to the current and voltage interharmonic subgroup amplitudes (Tables III and IV, respectively), all of the adaptive methods (the ARM, AEM, and APM) give lower values than those obtained by the IECM. Moreover, as expected, the results obtained using the subspace-based methods (the ARM and AEM) are similar in most cases.

Tables III and IV show that the IECM interharmonic subgroups have larger values than those obtained using the adaptive methods, confirming the absence of spectral leakage caused by the 11th and 13th harmonics.

The different processing techniques were also compared with an additional method based on the extension of IEC groupings to the high-resolution DFT spectral analysis performed on 3 s (IEC3sM) [11]. As an example, Fig. 9 compares the amplitudes of some harmonic and interharmonic subgroups obtained using the ARM, AEM, APM, IECM, and IEC3sM for the current analysis. From this figure, it appears that the problem of spectral leakage can partially be reduced by using the IEC3sM and that the results of the IEC3sM are closer to those obtained using the proposed methods.

C. Laser-Printer-Measured Waveform

The current and voltage waveforms are measured at the PCC of the LV network supplying a high-performance laser printer. The laser printer is a harmonic and an interharmonic source due to its time-varying absorption, which is asynchronous with the power-system frequency during the printing stage.

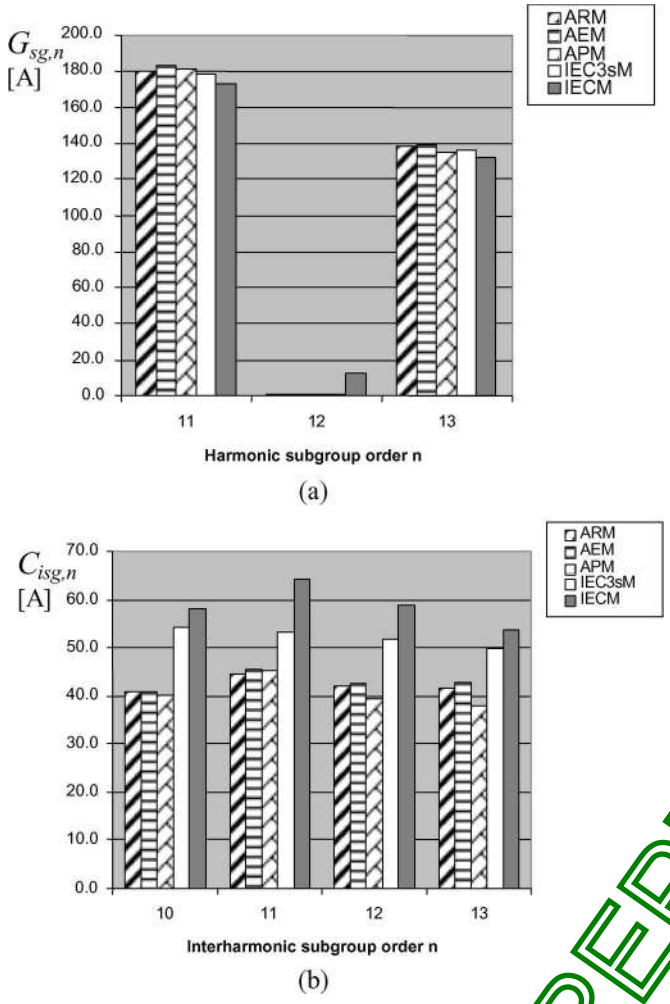

Fig. 9. DC arc-furnace current waveform. (a) Some harmonic and (b) interharmonic subgroup amplitudes.

TABLE V
LASER-PRINTER VOLTAGE WAVEFORM: HARMONIC SUBGROUP AMPLITUDES EVALUATED OVER 3-S INTERVAL USING THE DIFFERENT TECHNIQUES

	$G_{sg,3}$ [V]	$G_{sg,5}$ [V]	$G_{sg,7}$ [V]
IECM	2.98	5.02	3.27
ARM	2.80	6.04	4.52
AEM	2.98	5.70	3.39
APM	3.11	5.02	3.53

The measurement system is composed of a PXI instrumentation system produced by the National Instruments (model PXI-1020), which is equipped with a data acquisition board (model NI PXI-4472) having eight channels and 24-b resolution. The current and voltage transducers are a LEM CT25-T and a LEM CV 3-1000, respectively.

In order to compare the different adaptive techniques with the IEC method, the voltage waveform is analyzed. Tables V and VI report the most significant harmonic and interharmonic subgroups of the voltage waveform. The analysis of Tables V and VI confirms the same conclusions of the previous case studies; in particular, it should be noted that, with reference to the interharmonic subgroup amplitudes (Table VI), the IECM introduces subgroups (C_{isg4} and C_{isg6}) that are null for the adaptive methods.

TABLE VI
LASER-PRINTER VOLTAGE WAVEFORM: INTERHARMONIC SUBGROUP AMPLITUDES EVALUATED OVER 3-S INTERVAL USING THE DIFFERENT TECHNIQUES

	$C_{isg,1}$ [V]	$C_{isg,4}$ [V]	$C_{isg,6}$ [V]
IECM	1.14	0.19	0.10
ARM	0.95	0.00	0.00
AEM	0.94	0.00	0.00
APM	0.94	0.00	0.00

IV. CONCLUSION

This paper has proposed selected advanced spectrum estimation methods for the evaluation of harmonic and interharmonic groupings.

The techniques are based on the application of Prony, ESPRIT, and root-MUSIC methods to a number of short contiguous variable time windows inside the ten fundamental periods (imposed by the IEC standards as time intervals to which the groupings have to be referred). The number and the duration of these short windows were obtained by applying an adaptive algorithm based on the minimization of the waveform estimation error.

The application of the proposed techniques to test the defined waveforms, the waveforms derived from simulations of an actual plant, and the measured waveforms supplying a high-performance laser printer leads to the following main outcomes.

1) Even if characterized by simplicity, the IEC standards may suffer inaccuracy problems under conditions such as those characterized by fundamental and harmonic desynchronization within the time-window width.
2) The APM, AEM, and ARM methods do not suffer particular problems due to the spectral leakage phenomenon, even in very critical conditions, such as those characterized by harmonics and interharmonics whose amplitudes and/or frequencies are time varying.
3) The APM and AEM methods provide very good approximations for harmonic and interharmonic subgroup estimation and do not introduce spurious subgroups; the ARM has the same accuracy, except in the case of test waveforms with interharmonics.
4) The APM generally provides the best performance.

Eventually, even if the use of the IEC standard technique represents a compromise to achieve different goals, such as

the needs for accuracy, simplification, and unification, the proposed approach is particularly useful for its very high precision, specifically in the case of particularly complex signals. This high precision has also been shown in [17], where the advanced methods (in particular the adaptive Prony method) were compared with some DFT advanced methods that improved DFT measurement performance by reducing sensitivity to desynchronization problems. Moreover, in [17], it has been shown that the computational cost of these proposed methods is certainly higher than the DFT-based methods.

REFERENCES

[1] S. H. Jaramillo, G. T. Heydt, and E. O'Neill Carrello, "Power quality indices for aperiodic voltages and currents," *IEEE Trans. Power Del.*, vol. 15, no. 2, pp. 784–790, Apr. 2000.

[2] M. S. Kandil, S. A. Farghal, and A. Elmitwally, "Refined power quality indices," *Proc. Inst. Electr. Eng.—Gener. Transm. Distrib.*, vol. 148, no. 6, pp. 590–596, Nov. 2001.

[3] *General Guide on Harmonics and Interharmonics Measurements, for Power Supply Systems and Equipment Connected Thereto*, IEC Std. 61000-4-7, 2002.

[4] *Power Quality Measurements Methods, Testing and Measurement Techniques*, IEC Std. 61000-4-30, 2002.

[5] C. W. Therrien, *Discrete Random Signals and Statistical Signal Processing*. Englewood Cliffs, NJ: Prentice-Hall, 1992, pp. 614–655.

[6] P. Stoica and R. Moses, *Introduction to Spectral Analysis*. Englewood Cliffs, NJ: Prentice-Hall, 1997.

[7] A. Bracale, P. Caramia, and G. Carpinelli, "Adaptive Prony method for waveform distortion detection in power system," *Int. J. Electr. Power Energy Syst.*, vol. 29, no. 5, pp. 371–379, Jun. 2007.

[8] A. Bracale, P. Caramia, and G. Carpinelli, "Optimal evaluation of waveform distortion indices with Prony and rootmusic methods," *Int. J. Power Energy Syst*, vol. 27, no. 4, 2007.

[9] Z. Leonowicz, T. Lobos, and J. Rezmer, "Advanced spectrum estimation methods for signal analysis in power electronics," *IEEE Trans. Ind. Electron.*, vol. 50, no. 3, pp. 514–519, Jun. 2003.

[10] A. Bracale, G. Carpinelli, D. Lauria, Z. Leonowicz, T. Lobos, and J. Rezmer, "On some spectrum estimation methods for analysis of non-stationary signals in power systems—Part I: Theoretical aspects," in *Proc. 11th ICHQP*, Lake Placid, NY, Sep. 12–15, 2004, pp. 266–271.

[11] A. Bracale, G. Carpinelli, D. Lauria, Z. Leonowicz, T. Lobos, and J. Rezmer, "On some spectrum estimation methods for analysis of non-stationary signals in power systems—Part II: Numerical applications," in *Proc. 11th ICHQP*, Lake Placid, NY, Sep. 12–15, 2004, pp. 260–265.

[12] D. Gallo, R. Langella, and A. Testa, "On the processing of harmonics and interharmonics: Using Hanning window in standard framework," *IEEE Trans. Power Del.*, vol. 19, no. 1, pp. 28–34, Jan. 2004.

[13] D. Gallo, R. Langella, and A. Testa, "A self tuning harmonics and interharmonics processing technique," *Eur. Trans. Electr. Power*, vol. 12, no. 1, pp. 25–31, Jan./Feb. 2002.

[14] D. Gallo, R. Langella, and A. Testa, "Desynchronized processing technique for harmonic and interharmonic analysis," *IEEE Trans. Power Del.*, vol. 19, no. 3, pp. 993–1001, Jul. 2004.

[15] A. Bracale, G. Carpinelli, Z. Leonowicz, T. Lobos, and J. Rezmer, "Measurement of IEC groups and subgroups using advanced spectrum estimation methods," in *Proc. IMTC*, Sorrento, Italy, Apr. 2006, pp. 1015–1020.

[16] G. Carpinelli, F. Iacovone, A. Russo, and P. Varilone, "Chaos-based modeling of DC arc furnaces," *IEEE Trans. Power Del.*, vol. 19, no. 4, pp. 1869–1876, Oct. 2004.

[17] A. Bracale, G. Carpinelli, R. Langella, and A. Testa, "Accurate methods for signal processing of distorted waveforms in power systems," *EURASIP J. Appl. Signal Process.*, vol. 2007, no. 1, p. 174, Jan. 2007. Article ID 92191, DOI: 10.1155/2007/92191.

Antonio Bracale (M'04) was born in Naples, Italy, in 1974. He received the M.S. degree in telecommunication engineering from the University of Naples "Federico II" and the Ph.D. degree in electrical energy conversion from the Second University of Naples, Aversa, Italy, in 2002 and 2005, respectively.

He is currently with the Electrical Engineering Department, University of Naples "Federico II." His research interest concerns power quality.

Guido Carpinelli (M'92) was born in Naples, Italy, in 1953. He received the M.S. degree in electrical engineering from the University of Naples "Federico II" in 1978.

He became a Full Professor of industrial energy systems with the Università degli Studi di Cassino, Cassino, Italy, in 1990. He is currently with the Electrical Engineering Department, University of Naples "Federico II." His research interest includes electrical power systems.

Prof. Carpinelli is a member of the IEEE Task Force on Probabilistic Aspects of Power System Harmonics.

Zbigniew Leonowicz (M'03) received the M.Sc. and Ph.D. degrees in electrical engineering from Wroclaw University of Technology, Wroclaw, Poland, in 1997 and 2001, respectively.

He was awarded an Advanced Fellowship by the North Atlantic Treaty Organization in 2001. He spent this fellowship with the Technical University of Dresden, Dresden, Germany. From 2003 to 2004, he was a Research Scientist with the RIKEN Brain Science Institute, Saitama, Japan. Since 1997, he has been with the Electrical Engineering Department, Wroclaw University of Technology. His current research interests include modern digital-signal-processing methods applied to power-system analysis.

Tadeusz Lobos received the M.Sc., Ph.D., and Dr.Sc. (Habilitate Doctorate) degrees in electrical engineering from Wroclaw University of Technology, Wroclaw, Poland, in 1960, 1967, and 1975, respectively.

In 1976, he was awarded a Research Fellowship by the Alexander von Humboldt Foundation, Germany. He spent this fellowship with the Technical University of Darmstadt, Darmstadt, Germany. From 1982 to 1986, he was with the University of Erlangen–Nuremberg, Erlangen, Germany. Since 1960, he has been with the Electrical Engineering Department, Wroclaw University of Technology, where he became a Full Professor in 1989. His current research interests are in the areas of transients in power systems, control, and protection, particularly the application of neural networks and signal processing methods in power systems.

Dr. Lobos received the Humboldt Research Award, Germany, in 1998.

Jacek Rezmer received the M.Sc. and Ph.D. degrees in electrical engineering from Wroclaw University of Technology, Wroclaw, Poland, in 1987 and 1995, respectively.

He is currently with the Electrical Engineering Department, Wroclaw University of Technology. His primary professional interests lie in new signal processing methods for electric power-system analysis.